PRE-EXISTING SURFACE SCRATCHES PROMOTING FLAKING OF SHADOW CORROSION ON BWR CLADDING

KARIN CARLING
Ringhals AB
SE-432 85 Väröbacka, Sweden

OLOF TENGSTRAND, ANNA-MARIA ALVAREZ
Studsvik
SE-611 82 Nyköping, Sweden

DAVID SCHRIRE
Vattenfall Nuclear Fuel
SE-169 92 Stockholm, Sweden

ABSTRACT

In the vicinity of nickel alloy spacers or other components, ”shadow corrosion” is seen on Zr-alloys in BWRs. This shadow corrosion oxide is prone to flake off the Zr-alloy cladding. These flakes have, more often than not, straight edges, and these edges often correlate to pre-existing axial scratches.
In this work, we have investigated the oxide on un-flaked and flaked areas, in and close to the axial scratches, with FIB-SEM. This method gives the possibility to explore cross-sections of the material with both high precision and high resolution.
In the paper the mechanisms behind shadow corrosion and the flaking oxide are discussed based on the results from the FIB-SEM-investigations.
There is an incentive for fuel vendors to avoid axial scratches in the manufacturing process since this is expected to reduce the risk of oxide flaking.

1. Introduction

1.1. Background: observed flaking of shadow oxide

Flaking of shadow oxide on BWR fuel cladding, where the edges of the flakes correlate with pre-existing surface scratches in the cladding surface, has been observed for various fuel designs manufactured by different vendors [1]. The phenomenon has been seen for fuel operated in different BWRs, under different operating conditions and widely differing water chemistry conditions. In some cases, the flaking takes the form of narrow strips of oxide with a thickness of up to 100 µm. Detailed inspection measurements showed that the strip-like flakes corresponded exactly to the spacing between pre-existing axial scratches in the cladding surface caused by the spacer contact during the fuel rod loading in the bundle manufacturing process. The scratches are clearly visible on the cladding (oxide) surface after operation, both in the shadow corrosion region as well as on surfaces without shadow corrosion, as long as the fuel rod surface is not covered with crud.

Localised flaking, especially if the oxide flakes are relatively thick, leads to local differences in the cladding temperature during operation. In the event that the bulk hydrogen content in the cladding is high enough, this can result in significant redistribution of hydrogen and the risk of high local hydrogen levels in the cooler locations where the oxide has flaked off. This in turn may have a negative impact on the cladding ductility, as well as leading to an increase in the local corrosion rate if a high volume fraction of hydrides is formed below the outer surface of the cladding.

1.2. Shadow corrosion under spacers

Increased corrosion occurs on Zr-base alloys in contact with or in close proximity to other metallic alloys in the reactor core radiation field in BWRs or other reactors with similarly oxidising water conditions. The oxide growth rate in the so-called shadow is typically accelerated compared to the oxide that forms on the Zr-base alloys in the same environment (temperature, water chemistry and radiation field) but without proximity to other metals. Shadow corrosion on the fuel cladding within the spacer region is normally observed in all BWR fuel, especially where the entire spacer is made of a Ni-base alloy.

The shadow corrosion rate is roughly inversely proportional to the distance between the corroding Zr-alloy and the "shadow-casting" other metal, resulting in a peak oxide thickness at the points of contact between the Zr-alloy and the other metal. Also, the shadow corrosion rate has been observed to decrease with time [2], although there is a paucity of shadow corrosion data from BWRs for times shorter than about 1 year of operation. This results in relatively thick oxide being formed already early in life, compared to the typical corrosion behaviour of modern BWR cladding outside of the shadow corrosion positions which tends to grow far more slowly until some acceleration may occur late in life.

Shadow corrosion is believed to be a form of radiation assisted galvanic corrosion, where the in-pile radiation fields are thought to play a critical role in elevating the conductivity of both the water and the zirconium oxide [2].

1.3. Role of cladding surface scratches in flaking of shadow oxide

Flaking of shadow oxide in connection with pre-existing surface scratches in the cladding surface has been found to occur without physical handling of the fuel rods, although additional flaking may occur if a fuel rod is removed from the assembly (which entails pulling the rod through the spacers while in contact with the spacer springs). Such flaking has even been observed where the shadow corrosion is not due to a spacer (in contact with the cladding) but due to an adjacent but non-contacting component [1].

The initial scratches in the cladding metal surface are typically shallower than the shadow oxide thickness. Since the oxide grows inwards from the surface into the cladding metal, the initial surface scratches in the metal should end up on the outer part of the oxide layer. However, it was not clear how the presence of relatively shallow scratches can affect the flaking of an oxide film that is far thicker than the depth of the scratches. The study presented in this paper was intended to elucidate the mechanism by which the surface scratches facilitate the flaking of the shadow oxide.

2. Experimental technique

It was decided to use a Focused Ion Beam (FIB) to mill out small cross-sections through the oxide layer, in the direction normal to the cladding wall surface, which could then be observed directly in a Scanning Electron Microscope (SEM). It was hoped that the images of the oxide sections at and adjacent to scratches, within and outside the shadow corrosion region, would provide sufficient information to deduce the way that the scratches interact with the oxide and affect the flaking process.

A Zeiss Auriga Cross Beam field emission SEM was used to obtain images using the SE2 detector for detection of secondary electrons. The built-in tilt-correction was applied to correctly image the cross-section surface. Ga+ ions were used for milling the FIB cross-sections. Different ion currents between 10 and 1 nA, all with acceleration voltage of 30 kV, were applied during the milling, with lower currents used nearer to the final lamella surface.

For the first FIB cross-sections a Pt strip was applied as a protective layer on the surface ahead of the milled section (e.g. see figure 2b and 3b). However, since the damage to the sample surface from the ion-beam was found to have no impact on the results for the current investigations, Pt was not applied for the later cross-sections. The main remaining artefact is the curtain effect seen as parallel vertical stripes on the exposed cross-section surface.

Since the FIB milling technique as applied in this way has a limited practical depth (of some tens of microns), it was decided to study a cladding sample with relatively little (and thin) shadow corrosion in order to include the entire oxide layer in the milled surface. For this reason, a cladding sample from a fuel rod, where the fuel assembly design gives only a very limited local proximity to the nickel-base alloy spring, was selected for the FIB-SEM. The cladding material is Zircaloy-2 and the fuel rod had been operated in the Forsmark 2 BWR to a rod average burnup of 50 MWd/kgU. The reactor operates with normal water chemistry, and with very low metallic impurity levels resulting in very low levels of crud. A half-ring of the cladding was cut out and defueled before mounting in a SEM holder with silver glue at one end for conduction.

3. Microscopy results

The visual appearance of the fuel rod (photographed in a periscope) at the position selected for the study is shown in Figure 1a. The SEM sample included the three axial scratch marks numbered 1-3 in the area with shadow corrosion; additionally another scratch (scratch 4) approximately 34° circumferentially away from scratch 1 and outside of the shadow corrosion area was also studied. Figure 1b shows an overview in the SEM of the flaked region of the sample. The red arrows indicate the FIB milling positions in the region of the flaked oxide.

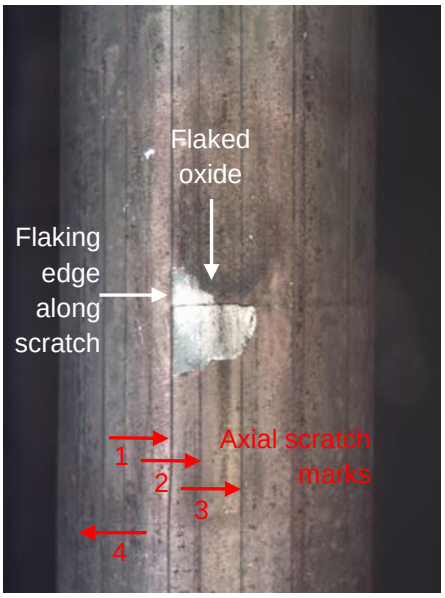

Figure 1a. Visual overview of rod with axial scratches and flaked shadow oxide.

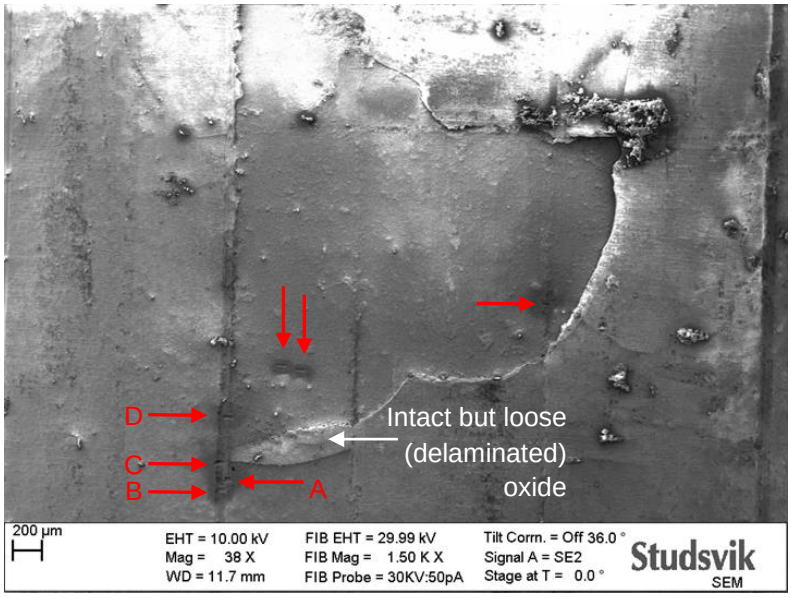

Figure 1b. SEM overview of sample indicating FIB milling cross-section (“ditch”) in region with flaked shadow oxide.

Several FIB cross-sections (or “ditches”) were milled adjacent to and in the scratch mark on the left hand side of the flaked-off oxide – these are numbered A to D and their positions are shown in Figure 1b. Since this scratch mark delineates the straight left edge of the oxide flake, the FIB ditches were milled out in a direction normal to the direction of the scratch in order to see how the oxide flaking was affected by the scratch mark. Ditches A to C are in the non-spalled region of the shadow oxide.

An overview of the scratch mark in the region with non-spalled oxide is shown in Figure 2a, together with the FIB ditch A on the right side of the scratch. The width of the scratch “valley” is approximately 80 µm and since the FIB ditches were limited to a width of about 30 µm it was not possible to have a single ditch extending right across the full width of the scratch valley. In Figure 2b it can be seen that the oxide on the side of the scratch valley is less than half as thick as the oxide just outside the scratch valley. It is also notable that the thicker oxide outside of the scratch valley has cracks parallel to the oxide-metal interface, while the thinner oxide on the side of the valley is essentially free of such cracks.

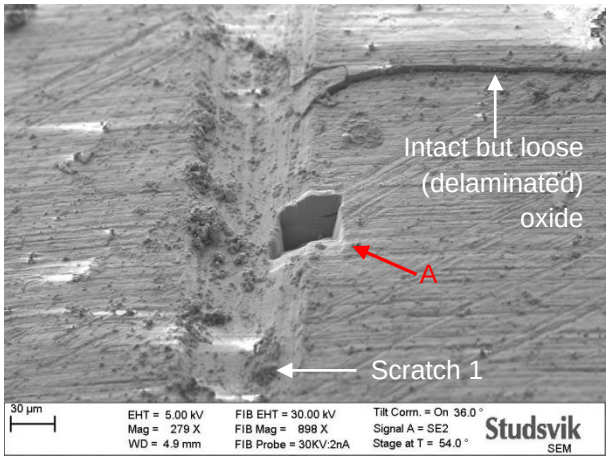

Figure 2a. Overview of scratch mark 1 and FIB ditch **A**.

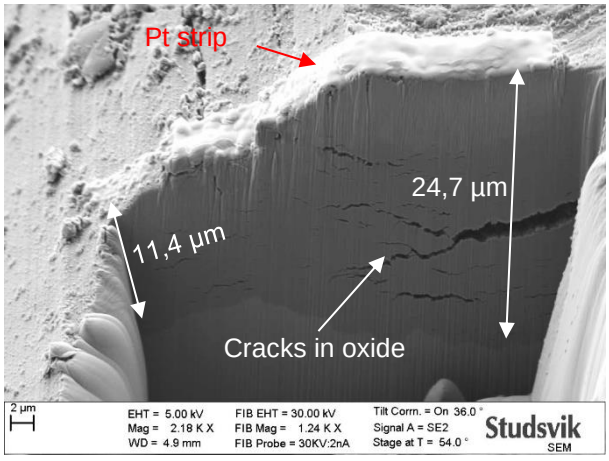

Figure 2b. FIB ditch **A**, higher magnification.

A position in the scratch mark 1 valley was selected for a FIB-milled ditch where cracks were seen emerging to the surface of the oxide layer in a direction parallel to the direction of the scratch. The intention was to see if the cracks emerging from the surface connect with cracks within the oxide layer parallel to the metal-oxide interface, which could explain the flaking.

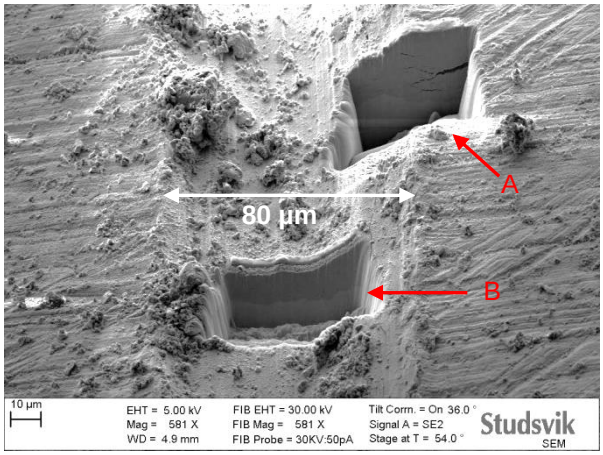

Figure 3a. Surface of scratch mark 1 valley showing positions of FIB ditches **A** and **B**.

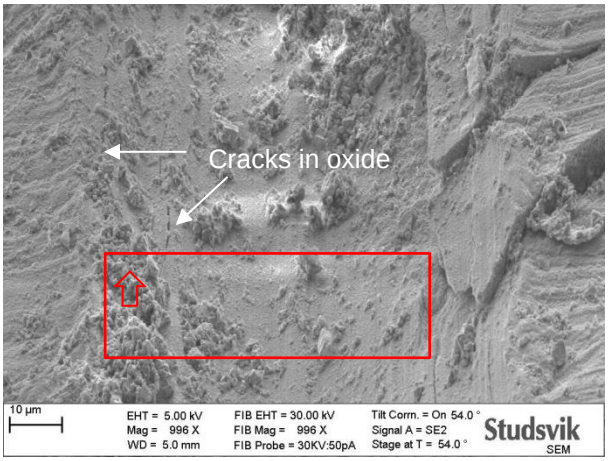

Figure 3b. Surface of scratch mark 1 valley before milling FIB ditch **C**. Arrow shows viewing direction in Figure 4a.

Figure 3b shows the surface of the scratch valley before milling the FIB ditch C (the position of ditch C is shown in the red rectangle). Figure 4a shows the FIB ditch C cross-section across almost the entire width of the scratch valley. The left half of this cross-section was milled a bit deeper and further to the left, to surface C' seen in Figure 4b which shows the

cross-section at the left side of the scratch valley, viewed from the direction shown by the red arrow in Figure 3b. In Figures 4a and 4b it can be seen that the cracks parallel to the direction of the scratch mark, which were seen emerging from the surface of the oxide prior to the FIB milling (shown by white arrows in Figure 3b), penetrate some way into the oxide layer in a direction normal to the surface (cracks 1 and 3 in Figure 4b). As seen in the cross-section, the oxide in the bottom (central part) of the scratch valley is far thinner (about 5 µm thick) than just outside the scratch (about 24 µm thick). A delamination-type crack parallel to the oxide-metal interface typically seen in the shadow oxide outside of the scratch region, is indicated as crack 2 in Figure 3b. This crack follows at roughly the same distance from the oxide-metal interface until almost reaching the surface where the oxide layer is thinnest in the central part of the valley.

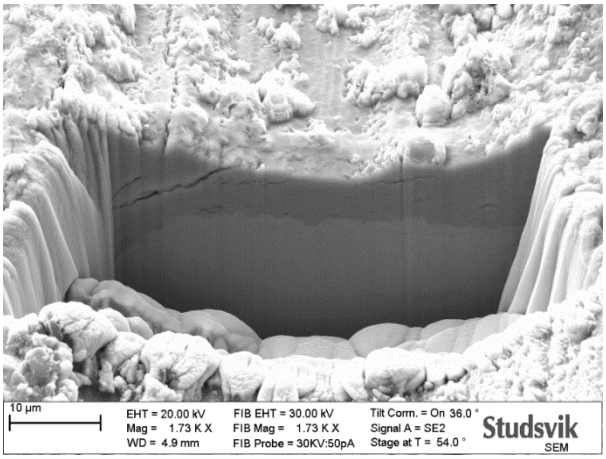

Figure 4a. FIB ditch **C** cross-section across scratch mark 1 valley.

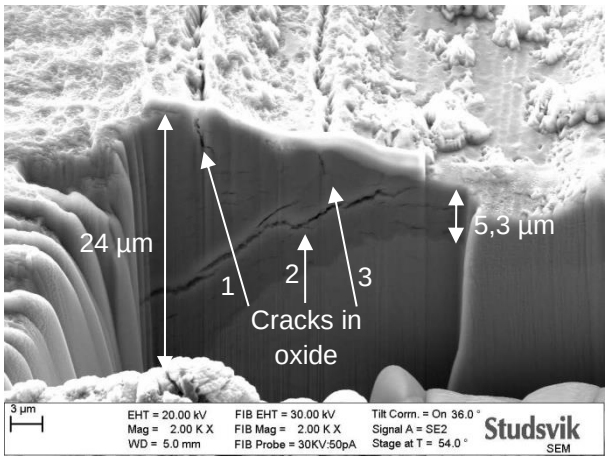

Figure 4b. Detail of FIB cross-section **C'**, left side with crack emerging to oxide surface.

The emergence of the delamination crack (crack 2) at the surface where the oxide thins, as well as the presence of long axial cracks vertically into the oxide layer (cracks 1 and 3) are considered the most important contributors to the flaking of the shadow oxide along the surface scratches.

The remaining question to be answered was why similar oxide layer flaking, with the edges of the flakes coinciding with the surface scratches, is not seen outside of the shadow corrosion region. In order to address this question, an additional FIB cross-section was milled across a surface scratch on the same cladding sample, but outside of the shadow corrosion area. The SEM sample only consisted of a half-ring of cladding, so the furthest position from the shadow oxide region practical for examination was at a scratch roughly 34º away in the circumferential direction from scratch 1, as indicated in Figure 1a. The position of the new FIB ditch E is shown in Figure 5a.

Figure 5b shows the FIB ditch C cross-section across almost the entire width of the scratch valley. The following features of the oxide in this cross-section are immediately seen to differ from the appearance of the oxide in the scratch valleys within the shadow corrosion area:

- The oxide layer has a uniform thickness and is relatively thick (about 20 µm) right across the bottom of the scratch valley. This oxide thickness corresponds roughly to the general oxide thickness measured on the cladding outside of the shadow corrosion position.
- The oxide appears to be dense, with few visible cracks, none of which are large.
- These small, short cracks are predominantly in the direction parallel to the metal-oxide interface but are fairly randomly distributed in the thickness direction.
- There is no single long delamination-type crack as seen in the other sections.

- There are no vertical cracks parallel to the scratch direction that emerge from the oxide outer surface. (In fact, no vertical cracks are seen at all).

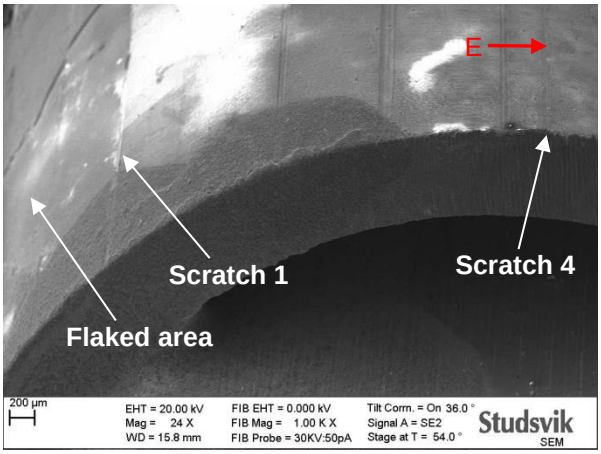

Figure 5a. Position of FIB ditch E outside of the shadow corrosion area.

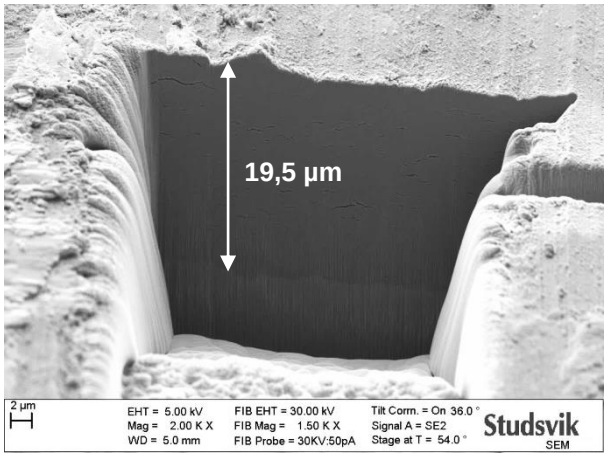

Figure 5b. FIB ditch E. Cross-section in middle of scratch 4 valley.

The very different appearance/morphology of the cracks in the oxide in this scratch valley, compared to those observed in the scratch in the area with shadow corrosion, appears to explain why no oxide flaking was seen in connection to scratches outside the shadow corrosion area.

4. Discussion

4.1. Oxide in/near scratches in the shadow corrosion region

Delamination-type cracks parallel to the oxide-metal interface were seen in the thicker shadow oxide outside of the scratch region, see Figures 2b and 4b. This type of de-cohesion or delamination crack is frequently seen in shadow oxide, and examples have sometimes been reported in the literature [3]. A previously unpublished example is shown in Figure 6 below, which shows a SEM image of a several mm long longitudinal section through the spacer shadow corrosion region of a different cladding sample. This sample is from a fuel rod with a different spacer design leading to more extensive shadow corrosion than in the cladding sample used for the FIB study. This example shows that a delamination-type crack parallel to the metal-oxide interface can extend over a very great distance without the oxide flaking off, in the absence of cracks in the radial direction penetrating through the oxide layer.

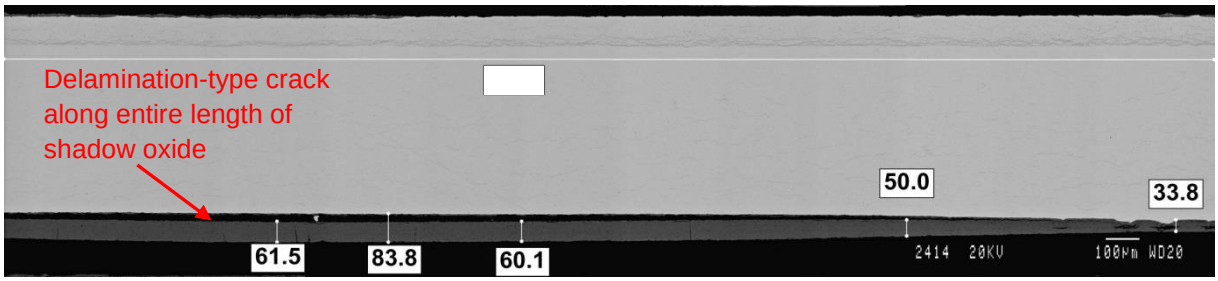

Figure 6. Longitudinal section through spacer shadow oxide region of a different cladding sample, showing delamination-type crack over an extensive distance. Markers indicate total distance from metal to the oxide outer surface including the crack width.

The scratch “valleys” in the cladding sample used for the FIB study are roughly 60 to 80 µm wide (Figures 3a and 3b). The oxide in the bottom of the scratch valley was much thinner

than on the sides of the valley and just outside the scratch (Figures 2b, 3a, 4a and 4b). Long shallow cracks in the cladding axial-radial direction (parallel to the scratch direction) penetrate a short distance vertically into the oxide layer. The emergence of the delamination-types cracks at the surface where the oxide thins, as well as the longitudinal cracks into the oxide layer which may penetrate as far as the delamination-type cracks, appear to be the cause of the flaking of the shadow oxide along the surface scratches.

4.2. Oxide in/near scratches outside the shadow corrosion region

Unlike the case for the scratch in the shadow corrosion region, the cross-section through a similar surface scratch outside the area that experienced shadow corrosion had a uniform oxide thickness across the entire scratch valley (Figure 5b), of the same thickness as the surrounding oxide layer outside the scratch. Neither delamination-type cracks or longitudinal axial-radial cracks along the length of the scratch were seen. Thus neither of the types of cracks believed to be responsible for the flaking along scratches inside the shadow corrosion region were observed, and the thinning of the oxide layer in the scratch did not occur either. Therefore none of the preconditions for flaking were present, which accounts for the fact that oxide flaking coincident with surface scratches has not been observed for any other forms of oxide than shadow corrosion.

4.3. Reason for thin oxide in scratches in shadow corrosion region

Having established that the large reduction in the oxide thickness on the surface of the scratch compared to the thickness outside the scratch apparently plays a role in the flaking mechanism, it is of interest to understand why the oxide is only thinner in the scratches in the area experiencing shadow corrosion. This possibility was in fact mentioned in a previous paper [1] before it was experimentally demonstrated in this study, based on the assumed galvanic nature of shadow corrosion.

In support of the hypothesis that shadow corrosion is in fact a form of galvanic corrosion, it has been pointed out that the electric field strength approaches zero at a corner of a conductor pointing away from an external electrode [4]. It was experimentally observed that the shadow corrosion oxide fell away to zero at the corner between the narrow diameter pin and the flat shoulder of the Zircaloy end plug of a BWR rod (where the pin is enclosed in a Ni-base alloy spiral spring), as seen in Figure 7. The spring, having a higher corrosion potential, is the external electrode in this case. Since the electric field is zero at the corner, the galvanic current density vanishes at this point. At all other locations the difference in corrosion potential between the two metals gives rise to a non-zero electric field (assuming the two metals are galvanically coupled).

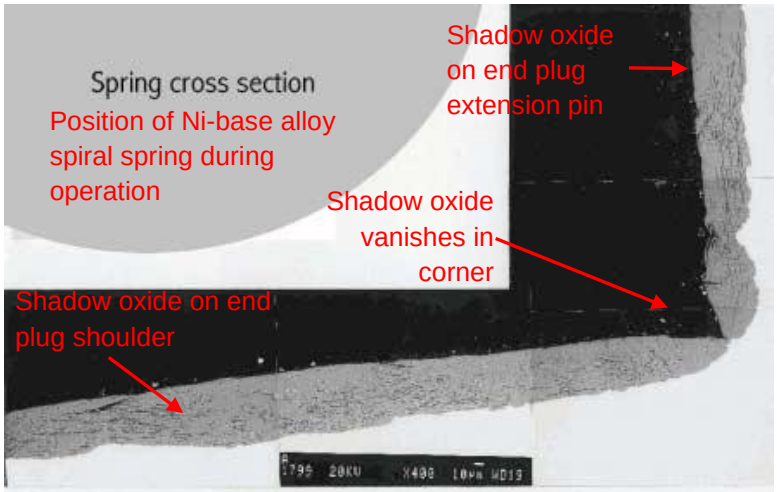

Figure 7. Section through the top end plug of a BWR fuel rod with a pin extension that fits within a spiral Ni-base alloy spring (from reference 4).

It is quite possible that the diminishing electric field due to the geometry of the surface scratches is the reason that the oxide layer inside the scratch is thinner than the surrounding oxide layer within the shadow corrosion area of the cladding. Since the uniform corrosion away from the shadow corrosion is not a galvanic type of corrosion, the geometry of the cladding surface (and its effect on an electric field) doesn't affect the corrosion rate.

In connection with the formation of the scratches in the original metal surface, it is likely that the subsurface material in and adjacent to the scratches undergoes significant plastic deformation and (at least in the case of recrystallized material) microstructural changes due to cold work. However, these local changes are the same for all the scratches, irrespective of whether or not they end up in areas of shadow corrosion. It therefore seems unlikely that these effects are the reason for the great reduction in oxide thickness in the scratches in the shadow corrosion regions but not elsewhere.

5. Conclusions

Flaking of shadow oxide on BWR fuel cladding, where the edges of the flakes coincide with pre-existing surface scratches in the cladding surface (typically caused by the spacer contact during the fuel rod loading in the bundle manufacturing process), has been observed for various fuel designs manufactured by different vendors [1]. Such scratches are seen on the cladding (oxide) surface after operation, both in the shadow corrosion region as well as on surfaces without shadow corrosion. However, oxide flaking coincident with the scratches has only been seen in the shadow corrosion region, even in cases where the shadow oxide is not very much thicker than the oxide outside the shadow region. Also, the coincidence of oxide flaking with surface scratches has not been observed or reported for PWR cladding in cases where widespread flaking of the oxide layer has been seen; shadow corrosion does not usually occur in PWRs.

In order to understand why this phenomenon occurs small cross-sections through the oxide layer have been milled by FIB and examined by SEM, at and near surface scratches inside and outside of the shadow corrosion region of a BWR cladding sample.

Based on the findings in this study, it is believed that the flaking of the oxide is facilitated by the fact that the oxide layer in the scratch "valleys" in areas subject to shadow corrosion is far thinner than the oxide layer outside of the scratches. The great reduction in thickness of the oxide layer in the scratch enables delamination cracks (i.e. cracks in the oxide parallel with the oxide-metal interface) to reach or approach the surface of the oxide on the sloping sides of the scratch valleys. When such a delamination crack meets with cracks that are formed normal to the oxide surface and travel longitudinally in the direction of the scratches (along the ridge of the edge of the scratch), an oxide flake becomes completely separated both from the underlying thin oxide layer attached to the metal and from the adjacent oxide along the longitudinal crack along the edge of the scratch.

Since the large difference in oxide thickness between the scratch and the surrounding surface only occurs in the case of shadow corrosion, this flaking detachment mechanism associated with the pre-existing surface scratches also only occurs where there is shadow corrosion. In the absence of shadow corrosion, the similarity in thickness of the oxide in the scratch and outside of the scratch counteracts the preferential separation of partially delaminated oxide layers at the edge of scratches.

References

1. D Schrire et al., “Flaking of shadow oxide on BWR cladding associated with pre-existing surface scratches”, Proc. TopFuel 2015, Zurich, Switzerland, 13-17 September 2015.
2. G Lysell, A-C Nystrand and M Ullberg, “Shadow Corrosion Mechanism of Zircaloy”, Proc. Zirconium in the Nuclear Industry: 14th International Symposium, ASTM STP 1467, 2005.
3. R B Adamson, D R Lutz and J H Davies, “Hot Cell Observations of Shadow Corrosion Phenomena”, KTG-meeting in Karlsruhe, Feb 29 to March 1, 2000.
4. G Lysell, A-C Nystrand and M Ullberg, “On the Shadow Corrosion Mechanism for Zirconium Alloys”, TopFuel 2001, Stockholm, Sweden.